AJNR

MRI of corpus callosal syndromes.

J T Curnes, D W Laster, T D Koubek, D M Moody, M R Ball and R L Witcofski

AJNR Am J Neuroradiol 1986, 7 (4) 617-622
http://www.ajnr.org/content/7/4/617

MRI of Corpus Callosal Syndromes

John T. Curnes[1]
D. Wayne Laster[2]
Terry D. Koubek[3]
Dixon M. Moody[2]
Marshall R. Ball[2]
Richard L. Witcofski[2]

Six patients, 6 to 13 years old, with corpus callosal abnormalities diagnosed by electroencephalography or CT were studied with a 0.15 T MR imager to determine the effectiveness of MRI in evaluating midline anomalies. Spin-echo images in the coronal, axial, and sagittal planes were obtained in two patients with Aicardi's syndrome and partial agenesis of the corpus callosum, in one patient with Dandy-Walker syndrome, and in two patients with septooptic dysplasia. Inversion recovery and spin-echo images were obtained in one patient with lipoma of the corpus callosum. Partial agenesis of the corpus callosum was seen in septooptic dysplasia, an association that has not been reported previously in the radiologic literature. Direct sagittal and coronal MRI provided better anatomic visualization of the brain and ventricles than did reformatted CT. T1-weighted images are sufficient to diagnose and delineate the extent of midline cerebral abnormalities. The unique capability of direct sagittal imaging makes MRI the best procedure for evaluating corpus callosal and other midline abnormalities.

Agenesis of the corpus callosum may be an isolated lesion or it may be associated with other central nervous system abnormalities. Cranial CT reveals the spectrum of agenesis of the corpus callosum (ACC); however, partial ACC resulting in little or no neurologic deficit may remain undetected on axial CT. We report six cases of complex midline developmental abnormalities with the common MRI finding of partial or complete ACC.

Subjects and Methods

A retrospective review of the medical records and MRI scans of three boys and three girls (median age 9 years) with corpus callosal abnormalities forms the basis of this study. A summary of the clinical data for each patient is given in Table 1.

Two patients were referred with clinical and electroencephalographic confirmation of Aicardi's syndrome. Two had hormonal, electroencephalographic, and clinical features characteristic of septooptic dysplasia including a small, pale, medially flattened optic disk on funduscopic examination. One patient was referred with a diagnosis of lipoma of the corpus callosum determined by CT. One patient had a diagnosis of Dandy-Walker malformation based on CT.

MR images were obtained on a resistive-magnet prototype imager manufactured by Picker International (Highland Heights, OH) (Picker 1000) and operating at a frequency of 6.4 MHz with a magnetic field of 0.15 T (1500 G). A 30-cm aperture was used. Spin-echo (SE) imaging was performed in three planes: axial (TR = 3000 msec, TE = 80 msec), coronal (TR = 1000 msec, TE = 80 msec), and sagittal (TR = 450 msec, TE = 30 msec). An inversion recovery (IR) pulse sequence with a 1400-msec TR and a 400-msec inversion time (TI) was used in one patient. Patients were studied with either four, eight, or 16 contiguous 1-cm slices. Two pulse averages were obtained. Images were generated by filtered-back projection of two-dimensional Fourier transform with a 256 × 256 matrix.

Received August 9, 1985; accepted after revision January 9, 1986.

[1]Department of Radiology, University of North Carolina School of Medicine, Chapel Hill, NC 27514.

[2]Department of Radiology, Bowman Gray School of Medicine at Wake Forest University, 300 S. Hawthorne Rd., Winston-Salem, NC 27103. Address reprint requests to D. W. Laster.

[3] Holmes Regional Medical Center, 1350 S. Hickory St., Melbourne, FL 32901.

AJNR 7:617–622, July/August 1986
0195–6108/86/0704–0617

TABLE 1: **Clinical Data and MRI Findings in Corpus Callosal Syndromes**

Case No.	Age	Gender	Diagnosis	Corpus Callosal Abnormality	Associated Abnormalities
1	6	F	Aicardi's syndrome	Partial agenesis	Dandy-Walker variant
2	8	F	Aicardi's syndrome	Partial agenesis (deficient splenium)	None
3	13	M	Lipoma of corpus callosum	Complete agenesis	Lipoma
4	12	M	Septooptic dysplasia	Partial agenesis	Small optic nerves, absent septum pellucidum, primitive optic ventricle
5	8	M	Septooptic dysplasia	Partial agenesis	None
6	10	M	Dandy-Walker malformation	Complete agenesis	Dandy-Walker malformation

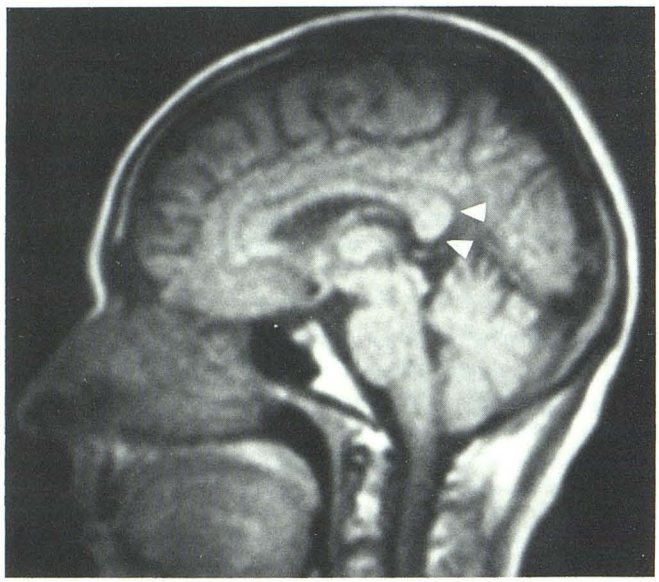

Fig. 1.—Normal subject. Sagittal midline MR SE 450/30. Notice bulbous configuration of a normal splenium of corpus callosum (*arrowheads*).

Results

The MRI findings in this study are summarized in Table 1. Axial SE 3000/80 sections provided little information because of the lack of contrast between the cerebrospinal fluid and the brain. Sagittal SE 450/30 images best demonstrated abnormality of the corpus callosum (Figs. 1–7). Two cases showed complete ACC, and four had varying degrees of partial ACC. Sagittal images also demonstrated the primitive optic ventricle in one patient with septooptic dysplasia (Fig. 5B), absence of the massa intermedia (Fig. 5B), and two Dandy-Walker cysts (Figs. 2A and 7A). Sagittal images revealed a radial arrangement of the sulci on the medial hemisphere in three cases (Figs. 2A, 4B, and 7A). In one case of Aicardi's syndrome, a subtle deficiency of the splenium of the corpus callosum with secondary enlargement of the quadrigeminal plate cistern was visible only on sagittal views (Fig. 3). Transaxial and coronal images were normal. Coronal SE 1000/80 images were most useful in evaluating the relationships of the interhemispheric fissure to the lateral ventricles, and the suprasellar cistern to the optic chiasm, and also the presence or absence of the septum pellucidum (Figs. 5A and 6A).

Lipoma of the corpus callosum, having a short T1, was seen well on both SE 450/30 and IR 1400/400 images (Figs. 4B and 4C); however, only CT demonstrated its peripheral calcification (Fig. 4A).

Discussion

Aicardi's Syndrome

The clinical features of Aicardi's syndrome were initially described in 1965 and consist of seizures, ACC, and ocular abnormalities [1]. Approximately 100 cases have been reported [2]. The original neuroradiologic investigation was by pneumoencephalography, which demonstrates corpus callosal abnormalities and occasional heterotopias in the periventricular region [3, 4]. Several reports of CT evaluation of Aicardi's syndrome have been published [3–6]. The association of Dandy-Walker syndrome with this abnormality has also been described (Fig. 2) [4].

Total or partial ACC is a universal finding in Aicardi's syndrome (Figs. 2 and 3) [2]. The primitive corpus callosum forms just dorsal to the lamina terminalis and develops in a rostrocaudal progression with the splenium maturing last [5, 7]. Total ACC malformation occurs before the 12th week of gestation, whereas deficiencies of the splenium or body of the corpus callosum occur between the 12th and 20th gestational weeks [5].

In one of the two cases of Aicardi's syndrome reported here, partial ACC manifested as a splenium lacking its normal

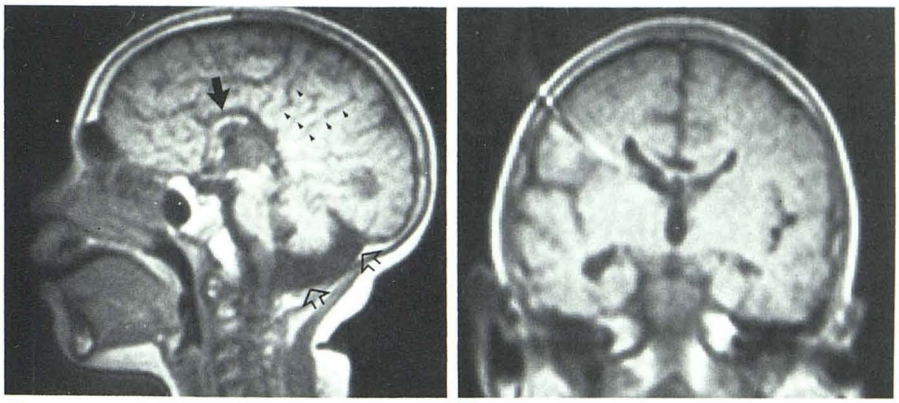

Fig. 2.—Case 1. Aicardi's syndrome. **A**, Sagittal midline MR SE 450/30. A thin vestige of hypoplastic corpus callosum is seen anteriorly (*arrow*). Its signal is slightly more intense than surrounding brain, indicative of myelinization. A radial arrangement of the sulci on medial surface of hemisphere can be seen posteriorly, where corpus callosum is completely absent (*arrowheads*). Note that sulci converge toward roof of elevated third ventricle. The Dandy-Walker variant is also well seen (*open arrows*), with hypoplasia of inferior and superior vermis, but torcula and straight sinus are in normal position. **B**, Coronal MR SE 1000/80. Lateral ventricles are widely separated and display a bicornuate appearance due to infolding of cingulate gyri and presence of longitudinal callosal bundles (of Probst). Superior aspect of third ventricle is interposed between the two lateral ventricles.

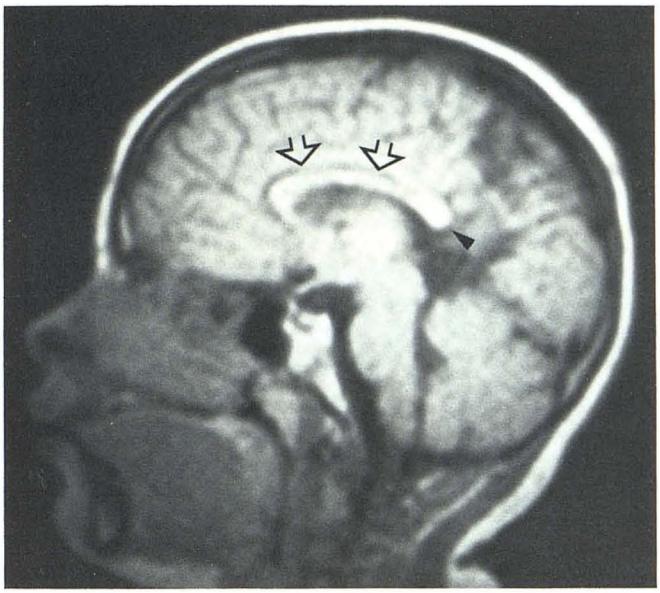

Fig. 3.—Case 2. Aicardi's syndrome. Sagittal midline MR SE 450/30. Hypoplasia of the splenium of corpus callosum is seen (*arrowhead*) with resultant enlargement of quadrigeminal plate cistern. *Open arrows* indicate pericallosal cistern.

bulbous configuration (Fig. 3). This anomaly is not discernible on axial or coronal MR or CT, but it is appreciated on direct sagittal MR images. The myelin-rich corpus callosum, with a short T1 time, is well demonstrated on sagittal SE 450/30 images. High contrast is achieved between the low-signal cerebrospinal fluid and the high-signal white matter.

Davidson et al. [8] have reported the MRI findings in two patients with partial ACC and three with complete ACC. They found involvement of the posterior body and splenium to be the greatest deficiencies in partial ACC. They calculated the corpus callosum/cerebrum ratio by measuring the greatest anteroposterior diameter of each structure. Both of their cases measured 0.26–0.27 (normal = 0.45), while one of our two cases of Aicardi's syndrome measured close to the normal ratio (0.40). However, the configuration of the splenium in our cases was abnormal, with tissue loss and resultant increase in size of the Galenic cistern.

Ben-Amour and Billewicz [9] studied the normal radiologic anatomy of the posterior cerebral vein, which surrounds the splenium. Normal measurements of this structure were important in the diagnosis of glioblastoma of the splenium. The average sagittal diameter of the splenium was 1.5 cm, with a maximum of 2 cm. In case 2, (Fig. 3), the splenium measures 8 mm in sagittal diameter, which falls well below the average found by Ben-Amour and Billewicz. Further studies are planned to evaluate the range of normal splenium width as seen on MRI. In addition, Kaufman et al. [10] have investigated the normal anatomic appearance of the corpus callosum. In their experience, the splenium always displays a bulbous configuration in patients without congenital abnormalities (Kaufman B., personal communication).

Lipomas

Lipomas of the corpus callosum are rare and easily visualized on CT because of their low attenuation values. Kushnet and Goldman [11] suggested that approximately one-half of these lipomas are accompanied by callosal agenesis. This is probably a conservative estimate, since partial ACC is difficult to diagnose even with CT. Other abnormalities associated with callosal lipomas include frontal bone defects, sphenoid encephaloceles, calcification of the walls of the lipoma, and heterotopic gray matter [12]. The peripheral curvilinear calcification in case 3 was well demonstrated on CT, but was undetected on MRI (Figs. 4A and 4C). This remains a serious limitation of MRI.

Corpus callosal agenesis in case 3 was well delineated by the sagittal SE 450/30 image (Fig. 4B). The short T1 signal on IR 1400/400 images, along with its characteristic midline location, confirmed the diagnosis of lipoma (Fig. 4C). The lipoma displayed the same high-intensity signal on both the SE 450/30 and IR 1400/400 images (Figs. 4B and 4C). Both pulse sequences have strong T1 weighting, which optimally characterizes the lipoma with its high fat content.

Radial arrangement of the gyri, seen in three cases, was best described by Probst [13] (Figs. 2, 4, 7). This abnormal

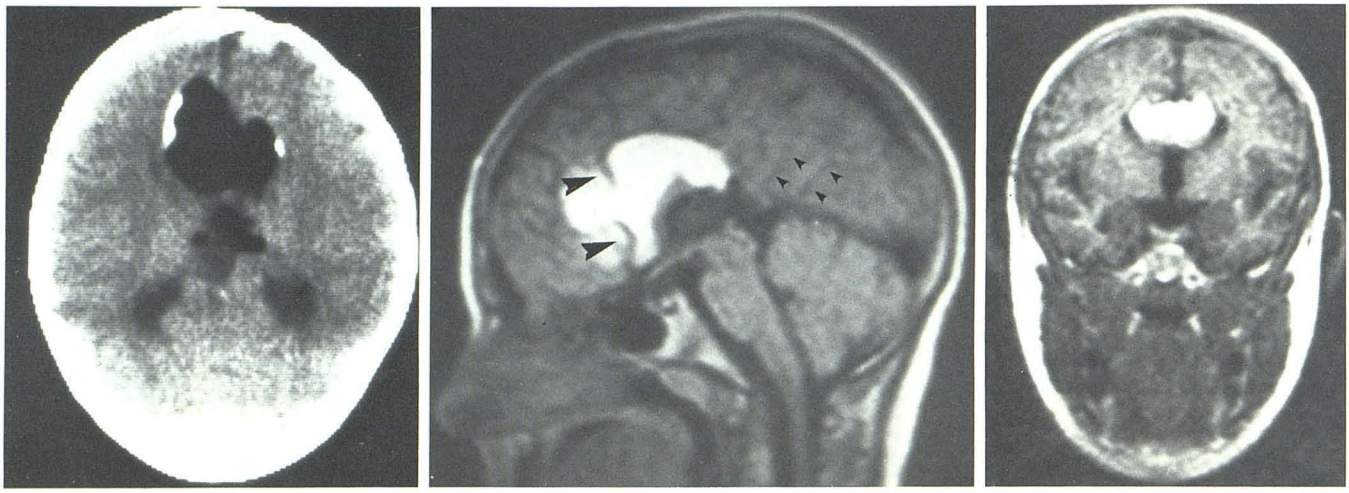

Fig. 4.—Case 3. Lipoma of corpus callosum. **A**, Axial CT. Midline lesion of fat density is present in expected location of genu of corpus callosum. Curvilinear calcification typical of a lipoma is also seen in this location. **B**, Sagittal midline MR SE 450/30. A large amorphous lipoma is located near body of corpus callosum and extends from top of third ventricle into pericallosal cistern and interhemispheric fissure. An anterior cerebral artery courses upward through mass (*large arrowheads*). The corpus callosum is absent, and there is radial arrangement of medial hemisphere gyri posteriorly (*small arrowheads*). **C**, Coronal MR IR 1400/400. Midline location of lipoma is well demonstrated. The characteristic splayed configuration of lateral ventricles can be seen.

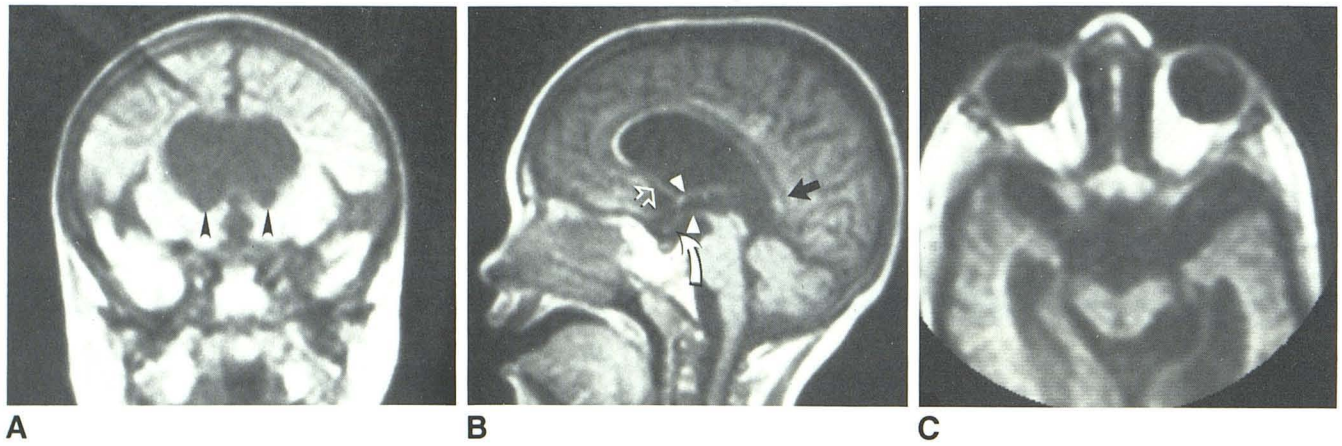

Fig. 5.—Case 4. Septooptic dysplasia. **A**, Coronal MR SE 1000/80. Arrested hydrocephalus is present, with ventricular enlargement but no transependymal absorption. Note bottom of interhemispheric fissure abuts roof of lateral ventricle. The squaring of top of lateral ventricle, the pointing of inferior aspect of lateral ventricles (*arrowheads*), and absence of septum pellucidum are classic pneumoencephalographic findings for septooptic dysplasia. **B**, Sagittal MR SE 450/30. Attenuation of corpus callosum is seen best on this image. Notice absence of normal bulbous configuration of the splenium (*black arrow*). Massa intermedia cannot be identified, but anterior portion of fornix is seen (*open arrowhead*). Notice primitive optic ventricle, which represents dilated optic recess of anterior third ventricle (*arrowheads*). The optic chiasm has a more vertical orientation than normal (*curved arrow*). **C**, Axial MR SE 450/30 at level of orbits. Both right (3 mm) and left (<3 mm) optic nerves are small and atrophic (normal ≥4.5 mm).

shape is thought to reflect the lack of formative influence of the corpus callosum.

The sonographic appearance of callosal agenesis was recently reported [14, 15]. Hernanz-Schulman et al. [14] present coronal and sagittal images, with pathologic correlation, of the multiple features of this malformation, including radial arrangement of the gyri. In addition, MRI shows that the sulci converge toward the roof of the elevated third ventricle, also described sonographically [15].

Septooptic Dysplasia

Septooptic dysplasia in another developmental midline abnormality that resembles milder forms of holoprosencephaly [16]. Both cases we report were in women, both had the clinical syndrome of hypothalamic dysfunction, and both had visual difficulty or blindness [17]. The initial radiographic characterization of this syndrome was by pneumoencephalography. Characteristic findings include absence of the septum

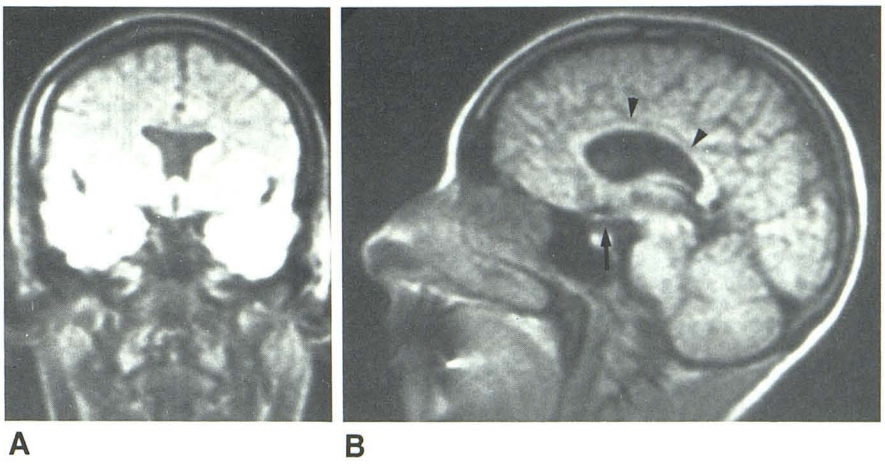

Fig. 6.—Case 5. Septooptic dysplasia. **A**, Coronal MR SE 1000/80. There is characteristic flattening of roof of lateral ventricles without evidence of septum pellucidum. Third ventricle appears normal in size. **B**, Sagittal MR SE 450/30. Third ventricle appears normal in configuration. The massa intermedia ia present. Body of corpus callosum is thinned, representing partial agenesis of corpus callosum (*arrowheads*), but splenium is present. Notice normally horizontal chiasm (*arrow*) (compare Fig. 5B).

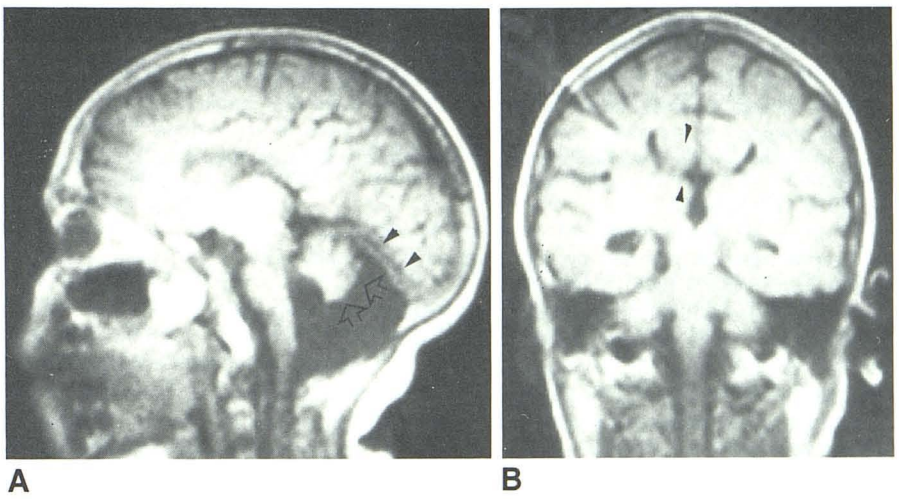

Fig. 7.—Case 6. Dandy-Walker cyst with agenesis of corpus callosum. **A**, Sagittal midline MR SE 450/30. There is agenesis with radial arrangement of medial hemispheric gyri. Elevation of straight sinus (*closed arrowheads*), continuity of fourth ventricle with cyst, inferior vermian agenesis, and superior vermian hypoplasia (*open arrowheads*) are noted. **B**, Coronal MR SE 1000/80. Typical appearance of agenesis of corpus callosum. Infolding of cingulate gyri and presence of lateral callosal bundles (of Probst) (*arrowheads*) give ventricles a batwing appearance.

pellucidum, squared frontal horns, enlargement of the suprasellar cistern, and persistence of the optic ventricle [18]. Plain films may reveal a small optic canal on one or both sides, and small optic nerves can be directly visualized with CT [17, 18, 19]. In addition, the chiasm is abnormally positioned and appears to divide in a vertical rather than a horizontal fashion [20].

Direct coronal imaging with MRI clearly delineates the findings previously noted on pneumoencephalography. The characteristic shape of the frontal horns, the slight widening of the third ventricle, and enlargement of the suprasellar cistern are displayed in Figures 5 and 6. The abnormal vertical configuration of the chiasm can be seen in Figure 5B. In addition, we have demonstrated a persistent, enlarged, primitive optic ventricle that is not seen on CT and was previously only a pneumoencephalographic finding (Fig. 5B) [18, 21].

In both patients with septooptic dysplasia, MR images in the axial plane showed hypoplastic optic nerves measuring ≦3 mm bilaterally (normal ≧4.5 mm). Coronal imaging through the optic nerves may further define their size and configuration.

A review of the literature revealed one description of ACC associated with septooptic dysplasia [18]. No previous radiographic demonstration of this association has been cited. Direct sagittal MRI in both cases of septooptic dysplasia shows clearly that the corpus callosum is not only attenuated and thin, but hypoplastic, particularly in the region of the splenium (Figs. 5B and 6B). It is probable that further MRI will reveal the association of corpus callosal abnormalities with septooptic dysplasia in a significant percentage of patients.

Dandy-Walker Syndrome

Agenesis of the corpus callosum is the most frequently noted coexisting anomaly in Dandy-Walker syndrome [22]. In case 6, sagittal MRI demonstrated the inferior vermian agenesis, the superior vermian hypoplasia, the continuity of the fourth ventricle with the Dandy-Walker "cyst," and the elevation of the straight sinus, in addition to ACC (Fig. 7). Before MRI, visualization of these features was limited, because sagittal CT reformation provides inadequate detail. An important role for MRI may be that of evaluating and differentiating

postfossa cysts; for example, extraaxial, megacisterna magna, Dandy-Walker variant (Fig. 2), and Dandy-Walker malformation (Fig. 7).

In summary, MRI is uniquely suited to the study of developmental defects involving the corpus callosum and other midline structures because of the capability for direct sagittal and coronal imaging. Sagittal and axial T1-weighted images were sufficient to diagnose and delineate the midline abnormalities described in our series. T2-weighted images were of little benefit. We believe that MRI will replace CT as the procedure of choice for the investigation of suspected midline abnormalities.

REFERENCES

1. Aicardi J, Lefebvre J, Lerique-Koechlin A. A new syndrome: spasm in flexion, callosal agenesis, ocular abnormalities. *Electroencephalogr Clin Neurophysiol* **1965**;19:606–612
2. Erenberg G. Aicardi's syndrome: report of an autopsied case and review of the literature. *Cleve Clin Q* **1983**;50:341–345
3. Bertoni JM, von Loh S, Allen RJ. The Aicardi syndrome: report of 4 cases and review of the literature. *Ann Neurol* **1979**;5:475–482
4. Phillips HE, Carter AP, Kennedy JL, Rosman NP, O'Connor JF. Aicardi's syndrome; radiologic manifestations. *Radiology* **1978**;127:453–455
5. Rothner AD, Duchesneau PM, Weinstein M. Agenesis of the corpus callosum revealed by computerized tomography. *Dev Med Child Neurol* **1976**;18:160–166
6. Dinani S, Jancar J. Aicardi's syndrome: (Agenesis of the corpus callosum, infantile spasms, and ocular anomalies). *J Ment Defic Res* **1984**;28:143–149
7. Larsen PD, Osborn AG. Computed tomographic evaluation of corpus callosum agenesis and associated malformations. *J Comput Tomogr* **1982**;6:225–230
8. Davidson HD, Abraham R, Steiner RE. Agenesis of the corpus callosum: magnetic resonance imaging. *Radiology* **1985**;155:371–373
9. Ben-Amour M, Billewicz O. The posterior cerebral vein. *Neuroradiology* **1970**;1:179–182
10. Kaufman B, Han JS, Huss R, et al. NMR of the normal/abnormal corpus callosum. Presented at the 22nd annual meeting of the American Society of Neuroradiology, Boston, June **1984**
11. Kushnet MW, Goldman RL. Lipoma of the corpus callosum associated with a frontal bone defect. *AJR* **1978**;131:517–518
12. Fujii T, Takao T, Ito M, Konishi Y, Okuno T, Suzuki J. Lipoma of the corpus callosum: a case report with a review. *Comput Radiol* **1982**;6:301–304
13. Probst FP. Congenital defects of the corpus callosum. *Acta Radiol [Suppl]* (Stockh) **1973**;331:1–152
14. Hernanz-Schulman M, Dohan FC Jr, Jones T, Cayea P, Wallman J, Teele RL. Sonographic appearance of callosal agenesis: correlation with radiologic and pathologic findings. *AJNR* **1985**;6:361–368
15. Atlas SW, Shkolnik A, Naidich TP. Sonographic recognition of agenesis of the corpus callosum. *AJNR* **1985**;6:369–375
16. Fitz CR. Holoprosencephaly and related entities. *Neuroradiology* **1983**;25:225–238
17. Wilson DM, Enzmann DR, Hintz RL, Rosenfeld G. Computed tomographic findings in septo-optic dysplasia: discordance between clinical and radiological findings. *Neuroradiology* **1984**;26:279–283
18. O'Dwyer JA, Newton TH, Hoyt WF. Radiologic features of septooptic dysplasia: de Morsier syndrome. *AJNR* **1980**;1:443–447
19. Manelfe C, Rochiccioli P. CT of septo-optic dysplasia. *AJR* **1979**;133:1157–1160
20. Fitz CR. Midline anomalies of the brain and spine. *Radiol Clin North Am* **1982**;20:95–104
21. Newton TH, Hoyt WF, Glaser JS. Abnormal third ventricle. In: Newton TH, Potts DG, eds. *Radiology of the skull and brain, vol 4, Ventricles and Cisterns*. St. Louis: Mosby **1978**:3481–3482
22. Lee SH, Rao KCVG. *Cranial computed tomography*. New York: McGraw-Hill **1983**:126